

Frequency conversion in laser-produced boron plasma using longitudinal pump scheme

R.A. Ganeev^a, M. Suzuki, M. Baba, and H. Kuroda

The Institute for Solid State Physics, The University of Tokyo, 5-1-5 Kashiwanoha, Kashiwa, Chiba 277-8581, Japan

Received 28 December 2004 / Received in final form 17 June 2005

Published online 16 November 2005 – © EDP Sciences, Società Italiana di Fisica, Springer-Verlag 2005

Abstract. The high-order harmonic generation from boron plasma was studied using the longitudinal pump scheme. The harmonics up to the 57th order ($\lambda = 13.96$ nm) were observed. The characteristics of plateau in the range of 15th to 57th harmonics were analyzed depending on fundamental radiation intensity and the saturation of harmonic cutoff was observed. The harmonic cutoff energy was restricted by the self-defocusing of femtosecond radiation. A comparison of longitudinal and orthogonal pump schemes of boron plasma excitation was presented.

PACS. 42.65.Ky Frequency conversion; harmonic generation, including higher-order harmonic generation – 42.79.Nv Optical frequency converters – 52.35.Mw Nonlinear phenomena: waves, wave propagation, and other interactions (including parametric effects, mode coupling, ponderomotive effects, etc.)

1 Introduction

The laser plasma has long been considered as a medium for harmonic generation [1,2]. These studies were carried out using gas jets at high ion concentration. A plateau-like shape of harmonic spectrum was observed in these studies. Another interesting opportunity of frequency conversion arises after the propagation of short laser pulses through the laser plasma produced at the surface of various targets [3–9]. However, the maximum observed harmonics generated at these conditions were limited to the 9th [6], 11th [5,7], 13th [4], 21st [8], and 27th [9] orders due to some concurred effects in high-excited multiple charged plasma. No plateau was observed in those studies.

The use of solid target ablation for HHG has some advantages with comparing to the gas jets (i.e., simplicity, gas saving, no differential pumping). The peculiarities of this approach with comparing to the conventional gas-jet technique include its capability of generating the media with higher density, longer length, and variable conditions. This technique also gives new degrees of freedom that can be used to optimize HHG. The use of any elements in the periodic table that can be formed as solid target may disclose many interesting opportunities for the generation of coherent XUV radiation.

Recently, we reported our studies on high-order harmonic generation (HHG) from the low-excited boron plasma using the orthogonal pump scheme [10]. We have demonstrated the generation of up to the 63rd harmonic

($\lambda = 12.6$ nm) of Ti:sapphire laser radiation. A steep decrease of the intensity of low-order harmonics was followed by a plateau pattern in the extreme ultraviolet (XUV) range.

Below we present our further studies of the HHG from low-excited boron plasma. In this paper, we demonstrate the HHG using the longitudinal pump scheme. The harmonics up to the 57th order ($\lambda = 13.96$ nm) were observed using this pump scheme. We discuss the difference in pump geometry and its influence on the HHG from laser plasma. We also analyze the restriction of harmonic generation due to the self-defocusing of main pulse in boron plasma caused by free electrons.

2 Experimental set-up

The 210-ps, 15-mJ, 796-nm prepulse from the uncompressed radiation of Ti:sapphire laser operating at 10 Hz pulse repetition rate was used for the excitation of boron plasma. This radiation was focused by a 200-mm focal length lens L1 into the hole of boron target T placed in the vacuum chamber (Fig. 1a).

The divergence of this radiation was increased using additional lens pair L2 to achieve a broad beam size (700 μm) in the focal plane of the focusing lens L1. The prepulse intensity at the target surface was varied in the range of $I_{pp} = 10^{10}$ W cm^{-2} to 10^{11} W cm^{-2} . The second beam ($t = 130$ fs, $E = 9$ mJ) was used as a main radiation interacted with boron plasma at different delays

^a e-mail: rashid.ganeev@yahoo.com

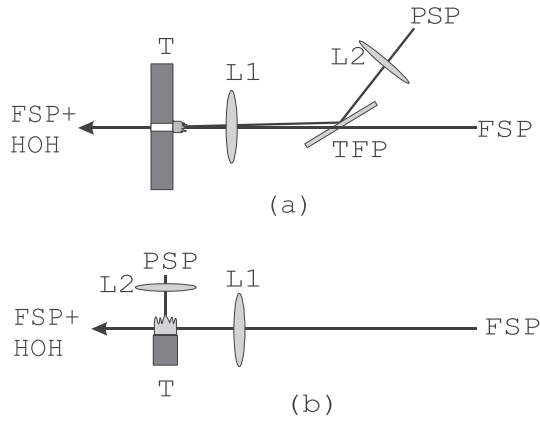


Fig. 1. Experimental set-up for (a) longitudinal and (b) orthogonal pump schemes of harmonic generation. T: boron target; L1, L2: focusing lenses; TFP: thin film polarizer; PSP: picosecond pulse; FSP: femtosecond pulse; FSP+HOH: femtosecond pulse and high-order harmonics.

relative to the picosecond pulses. The femtosecond main pulse was focused by a 200-mm focal length lens L1 from the longitudinal direction into the plasma with the maximum intensity of $I_{fp} = 2 \times 10^{15} \text{ W cm}^{-2}$. The beam waist diameter and confocal parameter of femtosecond radiation were measured to be $60 \mu\text{m}$ and 6 mm , respectively. This radiation and generated harmonics were propagated through the plasma and 0.5-mm hole drilled in 4-mm thick boron.

Low-order harmonics were analyzed using the vacuum monochromator (Acton Research Corporation, VM-502) and photomultiplier tube. High-order harmonics were analyzed by a flat-field grazing incidence XUV spectrometer [11] equipped with microchannel plate (MCP) and recorded by a CCD camera. A comparison of HHG in the cases of longitudinal and orthogonal pump schemes was carried out using experimental arrangements presented in Figures 1a and 1b.

3 Results and discussion

In the first set of experiments we analyzed the low-order harmonic generation using the vacuum monochromator. The 3rd harmonic conversion efficiency was measured to be 2×10^{-4} .

The heating radiation intensity on the target surface in these experiments was kept up at $10^{10} \text{ W cm}^{-2}$. The spectrum of boron plasma in the visible and UV ranges observed in these studies is presented in Figure 2.

We did not carry out the time-resolved spectral studies of plasma emission, so we could not assume that the main laser pulse interacting with the mixture of neutrals and singly charged boron up to the maximum delays used in our experiments (94 ns). Our temporal waveform studies of the integrated spectrum of boron plasma showed that the plasma emission disappearing during a period of 3 to 5 ns at the optimal prepulse intensity (Fig. 3).

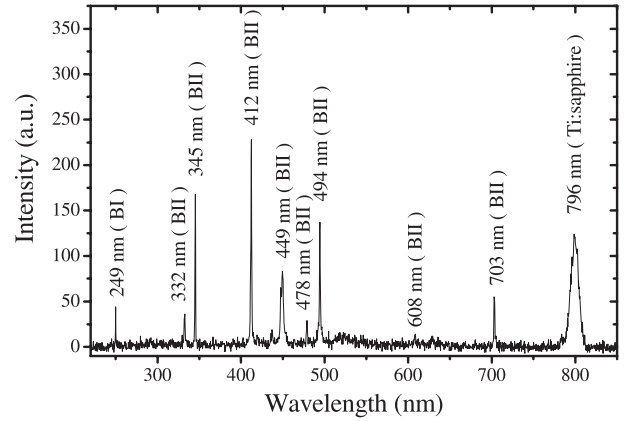


Fig. 2. Spectrum of boron plasma in the visible and UV ranges.

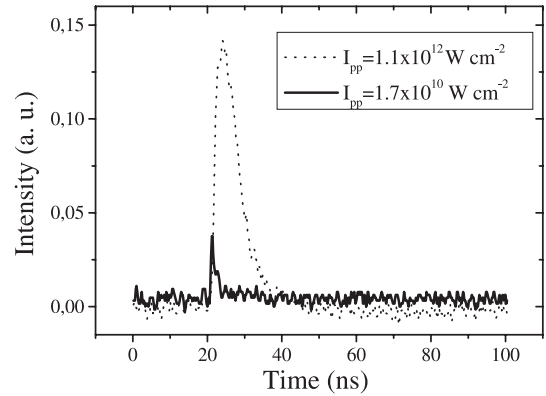


Fig. 3. Oscilloscope traces of boron plasma emission at different prepulse intensities.

The dependences of low-order harmonic output on femtosecond radiation intensity were close to the ones revealed from the theory of harmonic generation [12]. In particular, the slopes of intensity-dependent curves for third and fifth harmonics were close to 3 and 5, respectively. However, for higher harmonic orders the $I_{q\omega}(I_{fp})$ dependences did not obey the predictions of low-perturbation theory.

The heating picosecond radiation played a crucial role for the creation of the optimal conditions for harmonic generation. At small prepulse intensities, the $I_{q\omega}(I_{pp})$ dependences were obeyed to the scale low with a slope in the range of 3 to 4. However, with the growth of prepulse intensity (for $I_{pp} > 4 \times 10^{10} \text{ W cm}^{-2}$) we observed a saturation and considerable decrease of conversion efficiency. The saturation of conversion efficiency can be attributed to various processes related with high electron concentration in plasma (phase mismatching caused by free electrons, re-absorption of harmonic radiation, self-defocusing of main beam, etc.).

In the next set of harmonic studies we used a flat-field XUV spectrometer for the analysis of HHG in the spectral range below 60 nm. High harmonics up to the 57th order ($\lambda = 13.96 \text{ nm}$) were routinely observed in these

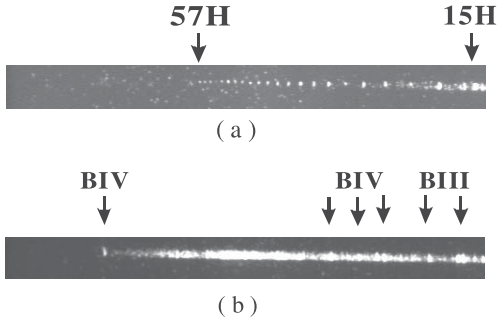


Fig. 4. Harmonic spectra and (b) boron spectra in XUV range measured at 13-ns delay and different intensities of prepulse radiation.

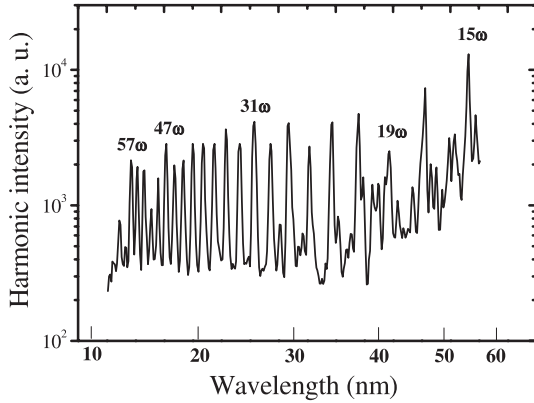


Fig. 5. Harmonic intensity as a function of the wavelength of generated XUV radiation.

experiments (Fig. 4a). The harmonics generated from boron plasma appeared to be analogous to the ones observed in gas-jet experiments with characteristic plateau-like harmonic distribution. The plateau and high harmonics disappeared in the case of higher intensities of prepulse radiation ($I_{pp} > 5 \times 10^{10} \text{ W cm}^{-2}$) causing the excitation of strong BIII and BIV lines (Fig. 4b).

The technique for the calibration of our data was as follows. We analyzed low-order harmonics using the “monochromator (Acton, VM502) + sodium salicylate + PMT” detection system. At the first step we calibrated the 3rd harmonic signal measured by this system using both known energy of the 3rd harmonic of 796-nm radiation generated in nonlinear crystals and 3rd harmonic generated from B plume. This calibration gave the absolute conversion efficiency for the 3rd harmonic generated from plasma to be 2×10^{-4} . The monochromator allowed observing the low-order harmonics up to the spectral range of 70 nm. Each of the next low-order harmonics was gradually decreased with coefficient of 4, and the conversion efficiency for the 9th harmonic (88.4 nm) was measured to be 3×10^{-6} . Then we observed the same 9th harmonic signal using the “XUV spectrometer + MCP + CCD camera” detection system. Figure 5 shows a part of harmonic spectrum generated from B plasma. It is seen that, starting from 21st harmonic, the spectrum shows a plateau pattern. For this shot, a conversion efficiency at the plateau

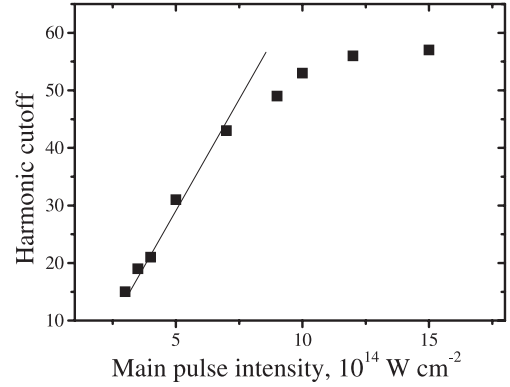


Fig. 6. Harmonic cutoff as a function of the main pulse intensity.

region was calculated to be 1×10^{-7} , taking into account the absolute conversion efficiency of 9th harmonic.

Our conclusion on plasma composition was drawn from the analysis of plasma emission in UV and visible ranges (see Fig. 2) at the conditions when maximum conversion efficiency of HHG was observed. However, the presence of higher charged ions was registered in some cases alongside with the XUV spectra of harmonics (Fig. 4a). Nevertheless, the optimal plasma composition was correlated with a dominance of the mixture of neutrals and singly charged ions.

We analyzed the influence of the delay between prepulse and main pulse on HHG conversion efficiency. No harmonics were observed at 2-ns delay. The harmonic yield was considerably increased 10 ns after the beginning of the interaction of prepulse with target. The difference between HHG achieved at 13-ns and 60-ns delays was insignificant. Further growth of delay led to the gradual decrease of HHG yield.

We carried out the studies of harmonic yield as a function of the polarization of main pulse. The efficient HHG was achieved only in the case of linear polarization, while no harmonics were observed in the case of circular polarization.

The appearance of plateau is a sign of the three-step model of HHG proposed in the early stages of high harmonic studies [13,14]. This mechanism predicts a cutoff energy of highest-order harmonic $E_c \approx I_{ip} + 3.2U_p$, where I_{ip} is the ionization potential of nonlinear medium, and U_p is the ponderomotive potential that showing the energy of electron in the field of electromagnetic wave. According to this model, the cutoff energy linearly depends on laser radiation intensity. Figure 6 presents the dependence between harmonic cutoff and main pulse intensity measured at 18-ns delay. This dependence showed a linear slope up to $I_{fp} \approx 7 \times 10^{14} \text{ W cm}^{-2}$. Further growth of intensity led to the decrease of a slope of $E_c(I_{fp})$ dependence. This process was associated with the variation of initial intensity due to the self-defocusing caused by free electrons generating during the propagation of femtosecond pulse through the boron plasma. This assumption was also confirmed during z -scan studies of boron plasma. The relatively low harmonic order at which the cutoff occurs

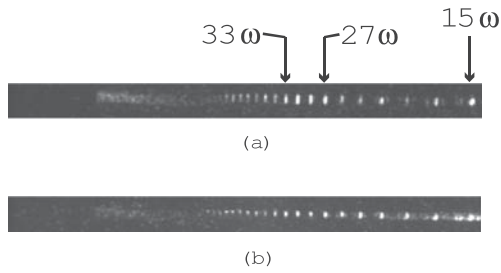


Fig. 7. Enhancement of 27th to 33rd harmonics yield in the case of (a) the orthogonal pump scheme with comparing to (b) the longitudinal pump scheme.

can also be caused by tunneling and barrier-suppressed ionization of the neutral boron already in the rising edge of the laser pulse. In that case the E_c is no longer determined by peak intensity, but by laser intensity at which the singly charged ions are further ionized.

The harmonic spectrum in the case of longitudinal pump scheme has shown a relatively smooth plateau (Figs. 5 and 7b). In the case of orthogonal pump scheme (Fig. 1b) the enhancement of harmonic yield for the 27th to 33rd orders was observed (Fig. 7a). The growth of intensity of some harmonics in plateau region observed using orthogonal scheme was probably caused by the enhanced phase matching conditions in this spectral range.

The difference in observed cutoff energies in the cases of longitudinal (57th harmonic) and orthogonal (63rd harmonic) schemes was insignificant. Our experiments were carried out at the conditions when the Rayleigh length (3 mm) of main beam was longer than the plasma size even at the delays of 30 ns. The focusing geometry is one of the main factors influencing the phase-matching conditions and HHG efficiency.

We carried out analogous studies using longitudinal scheme in the case of Mo target [15]. Those studies were performed at low-order harmonic spectral range (up to the 9th harmonic). We analyzed various parameters of this process and presented the quantitative measurements of harmonic yield at different delays, main pulse and prepulse intensities, as well as spectral and temporal measurements. The behavior of harmonic yield in the case of boron target was similar to Mo one, so we did not repeat the same measurements, but referred to our paper.

The reason of using a longitudinal instead of orthogonal pumping is to find the optimal conditions of the HHG in laser-produced plumes. The longitudinal pumping has both positive and negative features, so the analysis of HHG in such a scheme could disclose some advantages. In particular, the spreading of plasma plume in this case occurs in a thin channel drilled inside the target, which means the achieving of prolonged dense plasma.

All the harmonic peaks decreased in magnitude together as the plasma concentration was gradually reduced with a decrease of prepulse energy. If the high-order harmonics were produced by ions while the lower ones by neutral atoms, then the harmonics would expect to scale very differently with plasma density because of the change of coherence length arising from free electrons appearance.

These observations suggest that both low- and high-order harmonics observed in these studies appear from the same species.

The question arising from these studies is whether ions or neutrals are responsible for observed harmonic generation from surface plasma. Our spectral measurements of plasma emission confirmed that the laser plasma dominantly consisted on the neutrals and singly charged ions prior to the interaction with femtosecond pulse. However, during the interaction of this plasma with femtosecond pulses we observed a growth of the concentration of singly charged ions as well as generation of multiply charged ions. These ions appear during the propagation of a leading part of main pulse, since the ionization of most neutral atoms occurred at considerably lower intensities with comparing to the peak intensity of femtosecond pulse. Whether ions or neutrals become responsible for HHG depends on which mechanism is responsible for this process. If this mechanism is a three-step one, then we should conclude about the involvement of ions in this process since the neutrals can be responsible only for low-order harmonic generation.

A discussion about the influence of multiply charged ions on HHG should mostly be concentrated not on these species, because they do not participate directly in this process, but on the growing influence of free carriers appearing simultaneously with these ions. The role of the former species is crucial due to their influence on the propagation properties of femtosecond beam. As we have shown, the free carriers play a decisive role both in the restriction of cutoff energy and conversion efficiency.

A three-step model could not explain the observed results with neutrals involved in the HHG process. The maximum harmonic order that can be achieved is defined by an atomic ionization potential, which is rather low for used target (8.3 eV). For instance, this potential is lower than the Xe atom ionization potential with which one can only generate harmonics up to the 21st order. Neutral atoms evaporated by prepulse could then only generate the harmonics with a maximum order lower than that and certainly not up to the observed harmonic orders. If one considers the barrier suppression intensity for B atoms, one gets an intensity of $1.5 \times 10^{13} \text{ W cm}^{-2}$. Above this intensity all the atoms would be ionized and therefore neutral atoms can only generate harmonics with a maximum order of 5 ($E_c = I_{ip} + 3.2U_p \cong 10.4 \text{ eV}$). The calculations of saturation intensity ($5 \times 10^{14} \text{ W cm}^{-2}$) for singly charged ions, that was close to the observed saturation of the $E_c(I_{fp})$ dependence, confirm the consideration of ions as the main source of harmonics in these experiments.

4 Conclusions

The observation of high harmonic generation (up to the 57th order) after the propagation of femtosecond laser pulses through the boron plasma produced by prepulse radiation using the longitudinal pump scheme was reported. The steep decrease of the intensity of low-order harmonics was followed by a plateau pattern, and the conversion efficiencies were measured to be between 2×10^{-4} (for

third harmonic) to 10^{-7} (within the plateau region). The HHG appeared to be efficient in the case of neutral and singly ionized plasma when multiple charged ion and electron concentration was negligible. We discussed the difference of HHG in the cases of orthogonal and longitudinal schemes. We also analyzed the observed limitation of harmonic cutoff and attributed it to the self-defocusing of main pulse.

The authors thank Dr. T. Ozaki for the installation of MCP plate.

References

1. S. Meyer, H. Eichmann, T. Menzel, S. Nolte, B. Wellegehausen, B.N. Chichkov, C. Momma, Phys. Rev. Lett. **76**, 3336 (1996)
2. S. Bannerjee, A.R. Valenzuela, R.S. Shah, A. Maksimchuk, D. Umstadter, J. Opt. Soc. Am. B **20**, 182 (2003)
3. A.B. Fedotov, S.M. Gladkov, N.I. Koroteev, A.M. Zheltikov, J. Opt. Soc. Am. B **8**, 363 (1991)
4. Y. Akiyama, K. Midorikawa, Y. Matsunawa, Y. Nagata, M. Obara, H. Tashiro, K. Toyoda, Phys. Rev. Lett. **69**, 2176 (1992)
5. R.A. Ganeev, V.I. Redkorechev, T. Usmanov, Opt. Commun. **135**, 251 (1997)
6. K. Krushelnick, W. Tighe, S. Suckewer, J. Opt. Soc. Am. B **14**, 1687 (1997)
7. W. Theobald, C. Wülker, F.R. Schäfer, B.N. Chichkov, Opt. Commun. **120**, 177 (1995)
8. S. Kubodera, Y. Nagata, Y. Akiyama, K. Midorikawa, M. Obara, Phys. Rev. A **48**, 4576 (1993)
9. C.-G. Wahlström, S. Borgström, J. Larsson, S.-G. Pettersson, Phys. Rev. A **51**, 585 (1995)
10. R.A. Ganeev, T. Ozaki, M. Suzuki, M. Baba, H. Kuroda, Opt. Lett. **30**, 768 (2005)
11. R.A. Ganeev, T. Kanai, A. Ishizawa, T. Ozaki, H. Kuroda, Appl. Opt. **43**, 1396 (2004)
12. J.F. Reintjes, *Nonlinear optical parametric processes in liquids and gases* (Academic, New York, 1984)
13. J.L. Krause, K.J. Schafer, K.C. Kulander, Phys. Rev. Lett. **68**, 3535 (1992)
14. P.B. Corkum, Phys. Rev. Lett. **71**, 1994 (1993)
15. R.A. Ganeev, I.A. Kulagin, M. Suzuki, M. Baba, H. Kuroda, Opt. Commun. **249**, 569 (2005)